การออกแบบเชิงโมเลกุลของสีย้อมอินทรีย์แบบ D-2 (π-A) เพื่อเพิ่มประสิทธิภาพของเซลล์แสงอาทิตย์ชนิดสีย้อมไวแสง

Molecular Architecture of D-2 (π-A) Metal-Free Organic Dyes for Efficient Dye-Sensitized Solar Cells

ศราวุฒิ ต้นตะภา[1] วิเชียร แสงอรุณ[2] วิทยา อมรกิจบำรุง[3]

Received: October, 2014; Accepted: January, 2015

บทคัดย่อ

ได้มีการออกแบบโมเลกุลสีย้อมอินทรีย์แบบใหม่เพื่อประยุกต์ใช้เป็นเซลล์แสงอาทิตย์ชนิดสีย้อมไวแสง โดยการปรับโครงสร้างให้อนุพันธ์ Heteroanthracene เป็นหมู่ให้อิเล็กตรอน (Donor Group, D) ที่ประกอบด้วย 2 หมู่รับอิเล็กตรอน (di-(*π Conjugated-Acceptor, π-A*)) เรียกว่า D-2(*π*-A) ได้ศึกษาเชิงทฤษฎีเกี่ยวกับสมบัติทางโครงสร้างไฟฟ้า และทางแสงของระบบ D-2(*π-A*) นี้ ได้มีการปรับโครงสร้างที่สภาวะพื้นโดยใช้การคำนวณด้วยระเบียบวิธีทฤษฎีฟังก์ชันความหนาแน่นที่ระดับของทฤษฎี B3LYP/6-31G(d,p) และคำนวณสมบัติที่สภาวะกระตุ้นของระบบนี้โดยใช้การคำนวณด้วยระเบียบวิธีทฤษฎีฟังก์ชันความหนาแน่นที่ขึ้นกับเวลาที่ระดับของทฤษฎี CAM-B3LYP/6-31G(d,p) ได้มีการศึกษาผลกระทบในตัวทำละลายด้วย ผลจากการคำนวณเชิงทฤษฎีแสดงให้เห็นว่าระบบ D-2(*π-A*) ทั้งหมดสามารถใช้เป็นสีย้อมไวแสงได้โดยมีระดับพลังงาน HOMO และ LUMO ที่เหมาะสมกับระดับพลังงานของแถบการนำของ TiO_2 และศักย์ออกซิเดชันของ I^-/I_3^- ผลเหล่านี้ยืนยันได้ว่าเกิดการส่งและรับประจุได้

คำสำคัญ : ทฤษฎีฟังก์ชันความหนาแน่น; เซลล์แสงอาทิตย์ชนิดสีย้อมไวแสง; D-*π*-A, สีย้อมอินทรีย์

[1] *คณะวิทยาศาสตร์ มหาวิทยาลัยขอนแก่น*
[2] *คณะวิศวกรรมศาสตร์ มหาวิทยาลัยเทคโนโลยีราชมงคลอีสาน วิทยาเขตขอนแก่น*
[3] *ศูนย์วิจัยนาโนเทคโนโลยีบูรณการ คณะวิทยาศาสตร์ มหาวิทยาลัยขอนแก่น*
E - mail : vittaya@kku.ac.th

Abstract

A new series of metal-free organic dyes for dye-sensitized solar cell application was designed by considering the heteroanthracene dyes acting as an electron donor group (D) accompanied with di-(πconjugated (π)-acceptor (A)), namely D-2(π-A). The geometries, electronic properties, as well as optical properties of the D-2(π-A) systems were theoretically investigated. The ground state structures were optimized using the density functional theory (DFT) method at the B3LYP/6-31G(d,p) level of theory. The excited state properties of the system were performed by the time-dependent DFT method at the CAM-3LYP/6-31G(d,p) level of theory. The solvent effect was taken into account. The calculated results show that all the D-2(π-A) systems can be candidates as dye sensitizer while they possess HOMO and LUMO energy levels match to the energy level of conduction band of TiO_2 and oxidation potential of I^-/I_3^-. This is confirmed that spontaneous charge transfer and charge regeneration would be occurred.

Keywords : Density functional theory; Dye-sensitized solar cells; donor-π conjugated-acceptor; Organic dye

Introduction

As one of the most commonly used for alternative energy, dye-sensitized solar cells (DSSCs) are choice to fulfill some essential applications in the future. The DSSCs have been intensively investigated since the report of high-efficiency solar cell based on dye-sensitized colloidal TiO_2 films by O'Regan and Grätzel (O'Regan, B. and Gratzel, M., 1991). Consequential a low-cost and easily design, then the fabrications of DSSCs have attracted significant attention to take on the challenge. In particular, development to use the devices based on potential low-cost replacement to other technology is mainly caused. However, DSSCs are fabricated differently components such as conductive transparent grasses, molecular dye sensitizers, metal oxides, and electrolytes (Hagfeldt, A. et al., 2010). In this regard, one of the crucial parts in the DSSCs, dye sensitizers are now challenged by devices investigating at a molecular level. This focuses on organic dyes because of the dyes exhibit not only higher extinction coefficient, but also simple preparation and purification procedure. This indicates the promising perspective of organic dye classes.

Accordingly, Snaith reported (Snaith, H.J., 2010) that the current maximum efficiency of the best performing DSSCs is 13.4%, while the theoretical maximum achievable with near IR dyes is just above 30%. Recently, a progress has been reported in this field and a very large number of metal-free organic dyes have been developed and shown good power conversion efficiencies in DSSCs (Tarsang, R et al., 2014; Verbitskiy, E.V et al., 2014; Sirohi, R et al., 2012; Wu, C.G et al., 2013; Menzel, R et al., 2012). To optimize DSSC efficiency, many efforts have been made to change the different part of organic dyes. Generally, organic dyes containing an electron donor unit (D) and an electron acceptor unit (A) as well as separated by a π-conjugation bridge (π). The metal-free sensitizers are designed based on D-π-A, to achieve effective charge separation and transfer (Fischer, M.K.R et al., 2010; Kim, B.H. and Freeman, H.S., 2013; Chen, Z. et al., 2007). New architecture based on D-A-π-A metal-free organic sensitizers was designed and predicted any properties for guideline in experimental studies to fast screen new dyes-sensitized DSSCs (Ding, W.L et al., 2013; Ding, W.L et al., 2013).

According to di-π-conjugated spacers-linked anchoring architecture D-(-π-A)$_2$, the synthesis and characterization of this system for applications in dye-sensitized solar cells have been reported by Grisorio and co-workers (Grisorio, R et al., 2013). These results support the efforts aimed at the structural engineering of D(-π-A)$_2$ dyes to design new, more efficient and stable organic sensitizers. Due to architecture D-(π-A)$_2$ meets the results requirement, then this criteria read to design new for highly efficient dye-sensitizers.

Based on above considerations, the modification and investigation of new donor-π-acceptor type organic dyes bearing heteroanthracene as an electron donor (denoted as D), thiophene units as π-conjugated linker (denotes as π), and cyano-acrylic acid as an electron acceptor and anchoring part (denoted as A) have been interested as dye sensitizer for efficient DSSCs. It is difficult to obtain several geometry, electronic, and optical properties of the dyes designed by studying experiments. However, theoretical calculations can alternative to predict their properties of the dyes to apply for DSSCs. Due to the designed organic dyes are based on architecture D-2(π-A) as displayed in Figure 1. Thus, the structural, electronic, and optical properties of metal-free organic dyes have been investigated by the density functional theory method.

Computational details

The most stable structures of all dyes were optimized by using the density functional theory (DFT) calculations. These calculations were performed with hybrid density functional B3LYP and using 6-31G (d,p) diffuse basis set (Parr, R.G. and Young, W., 1989; Hohenberg, P. and Kohn, W., 1964; Khon, W. and Sham, L., 1965; Beck, A.D.J., 1993; Lee, C et al., 1988). For the single point energy calculations, the time-dependent density functional theory (TD-DFT) under the long-range corrected functional CAM-B3LYP (Yanai, T. et al., 2004) at the same level were used to calculate the vertical transition energies to the valence excited-states. Electronic densities of the highest occupied molecular orbital (HOMO) and the lowest unoccupied molecular orbital (LUMO) are calculated to show the position of the localization of electron populations along with the calculated energy level diagram. The bulk solvent effects in water, methanol, and ethanol phases were evaluated using the Conductor-like Polarisable Continuum Model (C-PCM) (Cossi, M et al., 2003; Cossi, M. and Barone, V., 2001; Barone, V. and Cossi M., 1998; Cossi, M et al., 1996). All calculations were performed with GAUSSIAN 09 program (Frisch, M.J et al., 2010).

Results and discussion

Geometries

The optimized ground-state structures and their selected geometry parameters of OSD and TSD dyes computed at B3LYP/6-31G (d,p) level are displayed in Figure 2. As shown, each dye molecule was consisted into three fragments; heteroanthracene acting as an electron donor (D), thiophene units acting as π-conjugated linker (π), and cyano-acrylic acid acting as an electron acceptor and anchoring part (A). For the purpose of comparison, the π-bride (n and m numbers of thiophene units from one to three units as showed in Figure 1) is affected for electron transfer consideration.

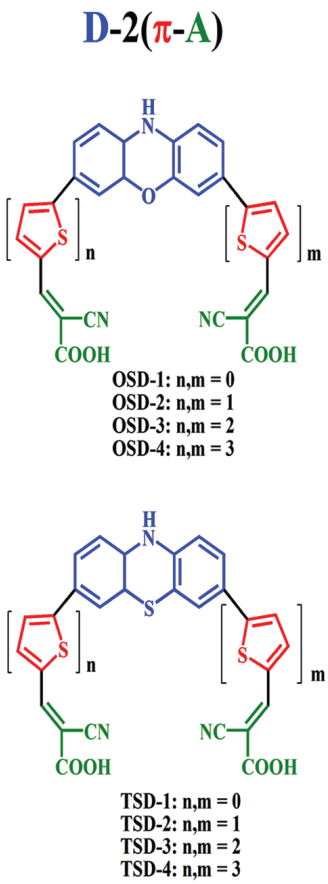

Figure 1 Modeled chemical structures of the dyes

To understand the structural planarity of the dye molecules, dihedral angle is importantly parameter to consideration the electron flow from D to A part. According to Figure 2, we observed that the symmetrical dihedral angles are not much differences in all structures. Considering the dihedral angles between D and π-bridge, optimized structures of all studied dyes showed that calculated dihedral angles are less than 2^{o} for the OSD-1 and TSD-1, indicating that the π-bridge is coplanar with cyano-acrylic acid. On the other hand, when the number of π-bridge parts is one to three units, the structural planarity of both OSD and TSD systems is significantly changed to form the deflection structures. These results confirm here that primary dihedral angle is more than 20 degree (Figure 2). In addition, trends of dihedral angle are differently decreased when increasing the linker bridge. However, the molecular coplanarity of π-bridge and electron acceptor unit can be effectively injected into the conduction band of TiO_2 through the anchoring group.

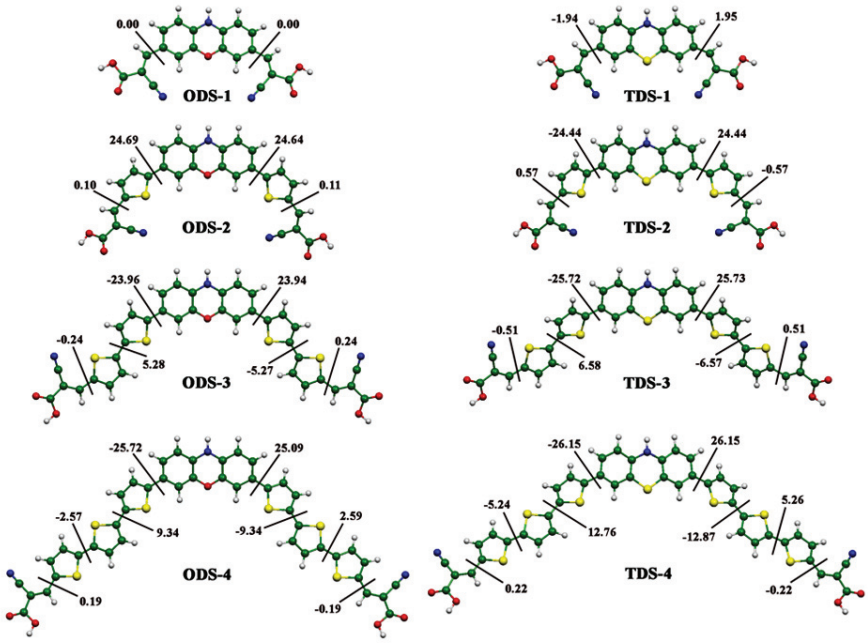

Figure 2 B3LYP/6-31G(d, p)-optimized structures of the dyes and their corresponding dihedral angle is lettered in degree

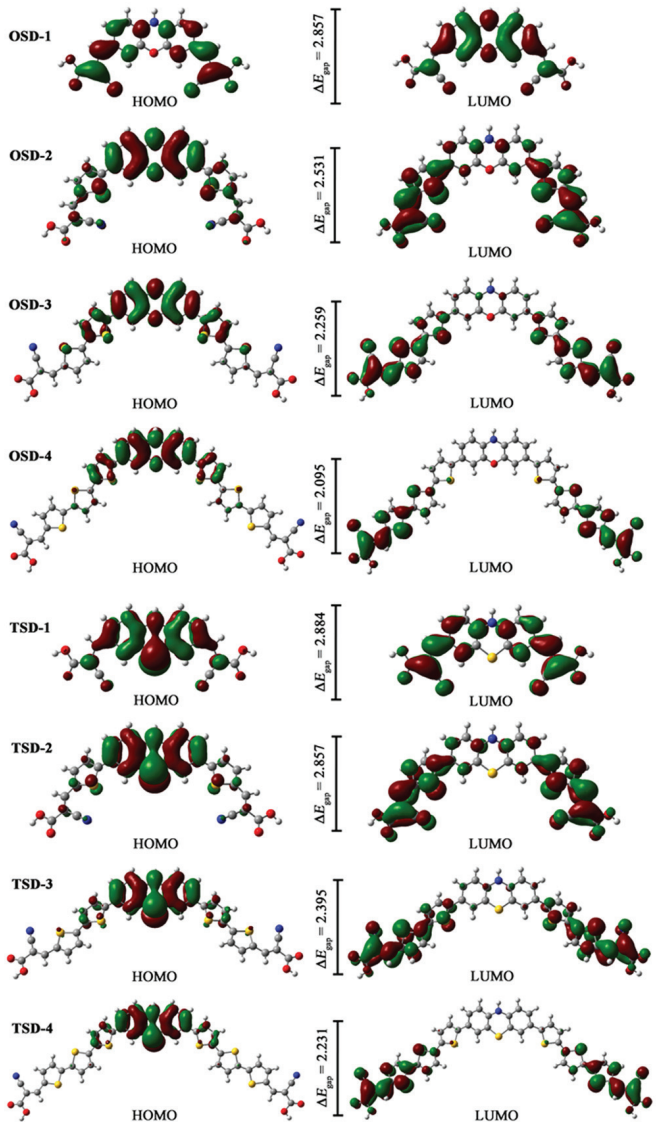

Figure 3 Frontier molecular orbitals of the dyes and their corresponding energy gap, ΔE_{gap} in eV

Frontier molecular orbitals and energy level diagram

The frontier molecular orbitals for the HOMO and LUMO are importantly characters to explain the mechanism of electron flows. The additional linker bridge unit effect on HOMO and LUMO orbitals is discussed. The LUMO level was just above the conduction band of TiO_2 semiconductor, while the HOMO level was below the iodine redox couple, leading to the criteria for good DSSC sensitizers.

The frontier molecular orbitals of the dyes computed at the B3LYP/6-31G(d,p) level of theory are displayed in Figure 3. As shown, the ground-state electron densities of HOMOs of all studied dyes are located on the donor parts. Whereas the LUMO electron densities of studied dyes are localized around the cyano-acrylic units, resulting efficient electron transfer from the excited state of the dyes to conduction band of TiO_2 semiconductor. In particular, both OSD-4 and TSD-4 dyes are distinctly appeared because of the cyano group (-C≡N) of acceptor units plays the strong electron withdrawing. Moreover, HOMO-LUMO energy gaps (ΔE_{gap}) of all studied dyes were computed and discussed. The values of ΔE_{gap} are also displayed in Figure 3. In detail, the ΔE_{gap} of the dyes is decreasing order OSD-1 > OSD-2 > OSD-3 > OSD-4. In the case of TSD dyes, trends of ΔE_{gap} are also occurred to OSD dyes. The calculated ΔE_{gap} of all studied dyes are observed in the ranges of 2.095-2.884 eV, resulting that the OSD-4 shows the minimum value of ΔE_{gap}, suggesting that the most linker bridge units are importantly affected onto molecular structures. This indicated that the narrow band gap is the result requirements for efficient DSSC sensitizers. In addition, observed ΔE_{gap} of the work are still narrowed comparing to TiO_2 semiconductor (energy gap of TiO_2 cluster is 3.13 eV) (Balanay, M.P. and Kim, D.H., 2008).

Furthermore, estimated schematic energy level diagram of related system is shown in Figure 4. According to the conduction band energy level (E_{CB}) of TiO_2 with the value of -4.00 eV (Asbery, J.B et al., 2001), and the redox couple of the electrolyte I^-/I_3^- of -4.8 eV (Ito, S et al., 2006) it is possible to view that the HOMO levels of derivative OSD and TSD dyes are located below the I^-/I_3^- redox potential and LUMO levels are above the conduction band of TiO_2. This is suitable for electron injection into the conduction band of TiO_2 as well. This can be understood that the intramolecular charge transfer from the molecular dyes to the TiO_2 through anchoring group. At the same time, the lose electrons of the oxidize dyes could be received electrons from redox potential of electrolyte. This is confirmed that spontaneous charge transfer and charge regeneration would be occurred. Moreover, it is concluded here that all the D-2(π-A) systems can be candidates as dye sensitizer while they possess HOMO and LUMO energy levels are well match to the energy level of TiO_2 conduction band edge and oxidation potential of electrolyte.

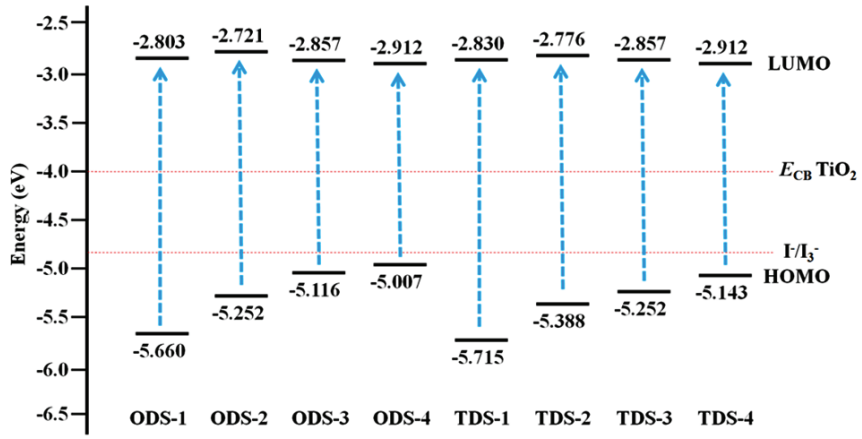

Figure 4 Schematic energy level diagram of the dyes, TiO_2 and electrolyte (I^-/I_3^-)

Absorption spectra and electronic transition properties

To understand the electronic properties, it is well know that TD-DFT/CAM-B3LYP functional is good choice to calculate their electronic properties. The C-PCM continuum salvation model was also used to calculate the solvent effects in this work.

In consideration for the UV-vis absorption spectra, as shown in Figure 5, the simulated absorption spectra observed peak in the visible region at around 380-570 nm. In the case of OSD dyes (Figure 5a), absorption spectra of OSD-1 to OSD-4 show the absorption maximum at 459, 486, 501, and 506 nm, respectively. Interestingly, the maximum of absorption of OSD-3 and OSD-4 dyes could be observed peak in about 60 nm red shift comparing to this of OSD-1. In addition, OSD-4 showed the highest absorption coefficients and broader absorption spectra of the peak. However, absorption spectra of TSD-1 to TSD-4 (Figure 5a) have quite similar results. For absorption spectra of both OSD and TSD dyes of the C-PCM (UAKS)/TD-DFT/CAM-B3LYP/6-31G (d,p) calculated in water and dichlorometane phases are shown in Figure 5b and 5c, respectively.

In order to understand the electronic transitions, the calculated transition energies of all studied dyes in methanol solvent are listed in Table 1, and their calculated transition energies in various different solvents are shown in Tables 2, 3 and 4. As listed, the vertical excitation energies, light harvesting efficiency (LHE), maximum absorption wavelength (λ_{max}), oscillating strengths (*f*) and transition characters of in the present are importantly factors in DSSC. In the first parameter, the calculated vertical excitation energies of the dyes are observed in the ranges of 2.451-2.861 eV (second column in Table 2). The vertical excitation energies are accordingly dependent on absorption peak. The absorption peak is at the lower excitation energy which was assigned as π-π^* transition of thiophene based π-conjugated linker.

Considering to the light harvesting efficiency (LHE), LHE is one of the key factors of the dye which is related to possible to maximize the photocurrent response. This LHE was evaluated by absorption energy of the dye. The LHE can be determined using the relations: (Sang-aroon, W et al., 2012; Sang-aroon, W et al., 2013; Irfan, A. and Al-Sehemi, A.G., 2012) LHE = $1\text{-}10^{-A}$ = $1\text{-}10^{-f}$ where A and f are the absorption and oscillating strength, respectively. As also listed in Table 3, the calculated LHE of the dye is increasing in order of OSD-1 < OSD-2 < OSD-3 < OSD-4. The longest dye OSD-4 has the highest LHE, resulting to the wavelength of maximum absorption of chromophoric group or conjugated bond of the dyes favors to LHE. Comparing to TSD dyes, trend of the term LHE has similar results to OSD dyes.

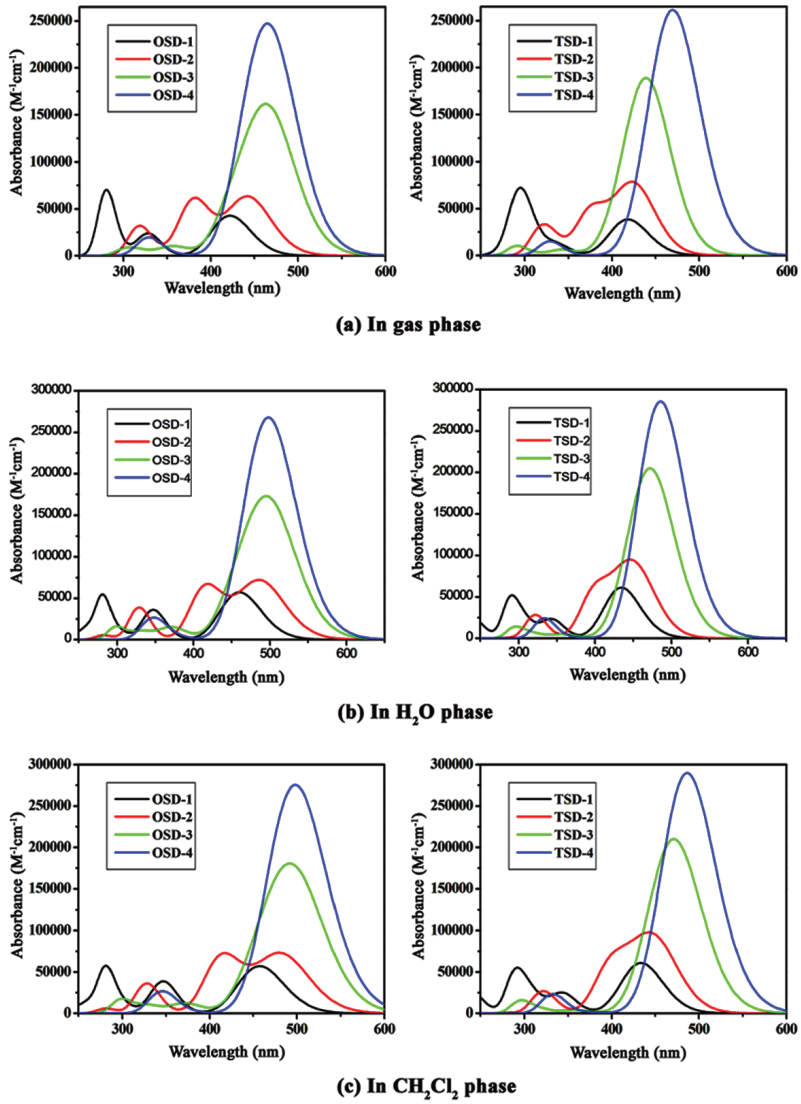

Figure 5 Simulated absorption spectra of all studied dyes

Table 1 The highest occupied molecular orbital energy (E_{HOMO}), the lowest unoccupied molecular orbital energy (E_{LUMO}), and HOMO-LUMO energy gap (ΔE_{gap}) of studied dyes computed at the B3LYP/6-31+G(d,p) level of theory

Dye	E_{HOMO} [a]			E_{LUMO} [a]			ΔE_{gap} [a]		
	gas	H_2O	CH_2Cl_2	gas	H_2O	CH_2Cl_2	gas	H_2O	CH_2Cl_2
OSD-1	-5.660	-6.368	-6.422	-2.803	-1.469	-1.497	2.857	4.898	4.925
OSD-2	-5.252	-5.987	-6.014	-2.721	-1.606	-1.606	2.531	4.381	4.408
OSD-3	-5.116	-5.823	-5.878	-2.857	-1.742	-1.742	2.259	4.082	4.136
OSD-4	-5.007	-5.742	-5.796	-2.912	-1.796	-1.796	2.095	3.946	4.000
TSD-1	-5.715	-6.531	-6.585	-2.830	-1.497	-1.524	2.884	5.034	5.061
TSD-2	-5.388	-6.232	-6.259	-2.776	-1.606	-1.606	2.612	4.626	4.653
TSD-3	-5.252	-6.041	-6.640	-2.857	-1.742	-1.742	2.395	4.299	4.898
TSD-4	-5.143	-5.932	-5.987	-2.912	-1.769	-1.796	2.231	4.163	4.191

[a] In eV.

Table 2 The vertical excitation energies, light harvesting efficiency (LHE), absorption wavelength (λ), oscillating strengths (f) and transition characters of all dyes in methanol phase computed at the TD/CAM-B3LYP/6-31G (d,p) level of theory

Dye	Energy [a]			λ [b]			*f*			Transition character [c]		
	gas	H_2O	CH_2Cl_2	gas	H_2O	CH_2Cl_2	gas	H_2O	CH_2Cl_2	gas	H_2O	CH_2Cl_2
OSD–1	2.939	2.697	2.713	421.9	459.8	457.0	0.5889	0.7892	0.7873	H→L (93%)	H→L (94%)	H→L (94%)
	3.779	3.574	3.579	328.1	346.9	346.4	0.3257	0.4980	0.5333	H→L+1 (90%)	H→L+1 (93%)	H→L+1 (93%)
	4.157	4.094	4.110	298.3	302.8	301.6	0.0495	0.1234	0.1313	H-1→L (54%)	H-1→L (71%)	H-1→L (71%)
	4.414	4.411	4.413	280.9	281.1	280.9	0.6847	0.2057	0.2238	H→L+2 (50%)	H-1→L+1 (40%)	H-1→L+1 (38%)
OSD–2	2.801	2.545	2.571	442.7	487.2	482.3	0.8605	0.9728	0.9769	H→L (80%)	H→L (82%)	H→L (82%)
	3.255	2.977	2.989	380.9	416.4	414.8	0.8365	0.9035	0.9711	H→L+1 (76%)	H→L+1 (80%)	H→L+1 (78%)
	3.808	3.719	3.712	325.6	333.4	334.0	0.1526	0.1225	0.1162	H-2→L (34%)	H-1→L+1 (36%)	H-1→L+1 (36%)
	3.928	3.790	3.800	315.7	327.1	326.3	0.3124	0.4229	0.3954	H-1→L (47%)	H-1→L (51%)	H-1→L (49%)
OSD–3	2.648	2.469	2.483	468.2	502.2	499.3	1.9859	2.0518	2.0952	H→L (61%)	H→L (63%)	H→L (62%)
	2.899	2.698	2.697	427.6	459.5	459.7	0.7419	0.8216	0.8485	H→L+1 (52%)	H→L+1 (57%)	H-1→L (31%)
	3.454	3.314	3.312	359.0	374.2	374.3	0.1273	0.1722	0.1456	H-2→L (29%)	H-2→L (31%)	H-2→L (31%)
	3.638	3.439	3.463	340.9	360.5	358.1	0.0241	0.0478	0.0326	H→L+2 (36%)	H→L+1 (37%)	H→L+1 (39%)
OSD–4	2.618	2.448	2.451	473.6	506.5	505.9	2.4843	2.5212	2.5464	H→L (42%)	H→L (42%)	H→L (41%)
	2.783	2.574	2.565	445.5	481.6	483.4	1.3681	1.4564	1.4903	H-1→L (39%)	H→L+1 (36%)	H-1→L (37%)
	3.336	3.131	3.129	371.6	396.0	396.3	0.0061	0.0065	0.0020	H→L+2 (33%)	H→L+2 (30%)	H→L+2 (31%)
	3.579	3.327	3.344	346.5	372.6	370.7	0.0169	0.0277	0.0144	H→L+1 (46%)	H→L+1 (49%)	H→L+1 (47%)
TSD–1	2.967	2.856	2.862	418.0	434.1	433.2	0.5303	0.8444	0.8398	H→L (92%)	H→L (93%)	H→L (93%)
	3.684	3.610	3.610	336.5	343.4	343.5	0.1578	0.3129	0.3347	H→L+1 (86%)	H→L+1 (90%)	H→L+1 (90%)
	4.007	4.004	4.010	309.4	309.6	309.2	0.2504	0.2473	0.2815	H-1→L (71%)	H-1→L (79%)	H-1→L (79%)
	4.198	4.264	4.259	295.4	290.8	291.1	0.7007	0.4725	0.4799	H-1→L+1 (35%)	H→L+2 (76%)	H→L+2 (77%)
TSD–2	2.917	2.753	2.766	425.0	450.4	448.3	1.0385	1.2204	1.2257	H→L (77%)	H→L (78%)	H→L (77%)
	3.293	3.096	3.095	376.6	400.5	400.6	0.6843	0.8124	0.8627	H→L+1 (72%)	H→L+1 (71%)	H→L+1 (69%)
	3.758	3.765	3.755	329.9	329.3	330.2	0.2375	0.1107	0.1042	H-2→L (33%)	H-1→L+1 (31%)	H-1→L+1 (30%)
	3.924	3.885	3.890	316.0	319.2	318.7	0.2869	0.3029	0.2919	H-1→L (36%)	H-1→L (41%)	H-1→L (39%)
TSD–3	2.806	2.606	2.611	441.9	475.8	474.9	2.3630	2.4601	2.4926	H→L (56%)	H→L (56%)	H→L (55%)
	3.015	2.773	2.765	411.3	447.2	448.5	0.5382	0.5963	0.6096	H→L+1 (48%)	H→L+1 (48%)	H→L+1 (47%)
	3.602	3.455	3.454	344.3	358.8	359.0	0.0832	0.0637	0.0494	H→L+2 (26%)	H-2→L (27%)	H-2→L (26%)
	3.818	3.612	3.631	324.7	343.3	341.5	0.0084	0.0104	0.0068	H→L+1 (41%)	H→L+1 (42%)	H→L+1 (43%)
TSD–4	2.616	2.533	2.530	474.0	489.5	490.0	2.8824	3.0271	3.0441	H→L (40%)	H→L (38%)	H→L (38%)
	2.743	2.624	2.612	452.1	472.5	474.6	0.9358	1.0373	1.0563	H-1→L (40%)	H-1→L (39%)	H-1→L (39%)
	3.366	3.299	3.292	368.4	375.9	376.7	0.0002	0.0090	0.0140	H→L+2 (36%)	H→L+2 (34%)	H→L+2 (35%)
	3.599	3.503	3.505	344.5	354.0	353.8	0.0007	0.0004	0.0021	H→L+1 (28%)	H→L+1 (38%)	H→L+1 (33%)

[a] In eV.; [b] In nm.; [c] Only major contribution to the transitions for each states are in parenthesis.

Table 3 Estimated light harvesting efficiency (LHE) of all dyes

Dye	LHE		
	gas	H_2O	CH_2Cl_2
OSD-1	0.742	0.838	0.837
OSD-2	0.862	0.894	0.895
OSD-3	0.990	0.991	0.992
OSD-4	0.997	0.997	0.997
TSD-1	0.705	0.857	0.855

Table 3 Estimated light harvesting efficiency (LHE) of all dyes (Cont.)

Dye	LHE		
	gas	H_2O	CH_2Cl_2
TSD-2	0.908	0.940	0.941
TSD-3	0.996	0.997	0.997
TSD-4	0.999	0.999	0.999

[a] In eV.

Table 4 The corresponding maximum absorption wavelength (λ_{max}) of all studied dyes computed at the TD-DFT/CAM-B3LYP/6-31G(d,p) level of theory

Dye	λ_{max} [a]		
	gas	H_2O	CH_2Cl_2
OSD-1	415.8	460.3	457.1
OSD-2	433.4	485.4	480.2
OSD-3	452.5	494.4	492.6
OSD-4	465.1	498.1	498.1
TSD-1	408.2	434.8	433.4
TSD-2	422.4	446.4	442.0
TSD-3	439.1	471.7	471.7
TSD-4	470.0	485.4	487.2

[a] In nm.

The corresponding maximum absorption wavelength (λ_{max}) of studied dyes in methanol solvent computed at TD-DFT/CAM-B3LYP/6-31G(d,p) level is also listed in Table 4. On the basic concept, the molecular dyes with broader absorption spectra and higher extinction coefficients have been expected to obtain the higher solar-to-electrical energy conversion efficiency (Gong, J et al., 2012). In calculation results, the λ_{max} of the D-2(π-A) systems are increasing in the order of OSD-1 < OSD-2 < OSD-3 < OSD-4. For TSD dyes, the λ_{max} of the D-2(π-A) systems are similar increasing in the order of TSD-1 < TSD-2 < TSD-3 < TSD-4. When comparing to calculate in gas phase, the λ_{max} observed in methanol is ~32-51 nm shifting from 416 → 457, 435 → 486, 458 → 501 and 474 → 506 nm for OSD-1, OSD-2, OSD-3 and OSD-4, respectively. However, the λ_{max} observed in water and ethanol is slightly different. Remarkably, for all D-2(π-A) systems, there are several absorption bands which are mainly observed in visible region.

In the last one key parameter, transition characters of studied dyes in methanol computed at TD-DFT/CAM-B3LYP/6-31G(d,p) level are also listed in Table 2. The transition characters are explained to electron movement between HOMOs to LUMOs which are dependent on the vertical excitation energies. Based on calculation results, transition characters of the dyes observed only major contribution that is the promotion of an electron from the HOMO → LUMO. In description results, the transition character from the HOMO to the LUMO (94%) is mainly controlled by vertical excitation energy of 2.704 eV. However, the majority of transition characters is decreasing in the order of OSD-1 > OSD-2 > OSD-3 > OSD-4. For TSD dyes, trend has similar result to OSD dyes. Furthermore, calculated transition characters of studied dyes in various different solvents are also reported.

Conclusions

A new series of metal-free organic for dye-sensitized solar cell application was designed by considering the heteroanthracene dyes acting as an electron donor group (D) accompanied with di-(π conjugated (π)-acceptor (A)), namely D-2(π-A). The geometries, electronic properties, and optical properties of D-2(π-A) systems were theoretically investigated. The ground state structures were optimized using the density functional theory (DFT) method at the B3LYP/6-31G(d,p) level of theory. The excited state properties of the system were performed by the time-dependent DFT method at the CAM-B3LYP/6-31G(d,p) level of theory. The solvent effect was taken by using C-PCM continuum model. Based on calculation results, the ΔE_{gap} of the D-2(π-A) dyes are observed in the ranges of 2.095-2.884 eV. However, the LUMO electron densities of studied dyes are localized around the cyano-acrylic units, resulting efficient electron transfer from the excited state of the dyes to conduction band of TiO_2 semiconductor. In addition, the D-2(π-A) dyes showed the higher absorption coefficients and broader absorption spectra of the peak, leading to higher solar-to-electrical energy conversion efficiency. All of the D-2(π-A) systems can be candidates as dye sensitizer while they possess HOMO and LUMO energy levels match to the energy level of conduction band of TiO_2 and oxidation potential of I^-/I_3^-. This is confirmed that spontaneous charge transfer and charge regeneration would be occurred.

Acknowledgement

The work is mainly supported by the National Research University Project, Khon Kaen University through the research Grant No. AFM-2553-Ph.d-07 and Advanced Functional Materials Cluster. The Integrated Nanotechnology Research Center, Department of Physics, Faculty of Science, Khon Kaen University is gratefully acknowledged for providing facilities. Also, the work is partially supported by the Institute of Research and Development, Rajamangala University of Technology Isan, and Faculty of Engineering, Khonkaen campus.

References

Asbery, J.B., Wang, Y.Q., Hao, E., Ghosh, H. and Lian, T. (2001). Evidences of hot excited state electron injection from sensitizer molecules to TiO_2 nanocrystalline thin films. **Research on Chemical Intermediates**. Vol. 27. pp. 393-406

Balanay, M.P. and Kim, D.H. (2008). DFT/TD-DFT molecular design of porphyrin analogues for use in dye-sensitized solar cells. **Physical Chemistry Chemical Physics**. Vol. 10. pp. 5121-5127

Barone, V. and Cossi M. (1998). Quantum Calculation of Molecular Energies and Energy Gradients in Solution by a Conductor Solvent Model. **Journal of Physical Chemistry A**. Vol. 102. pp. 1995-2001.

Beck, A.D.J. (1993). Density-functional thermochemistry. III. The role of exact exchange. **J Chemical Physics**. Vol. 98. pp. 5648-5652

Chen, Z., Li, F. and Huang, C. (2007). Organic D-π-A Dyes for Dye-Sensitized Solar Cell. **Current Organic Chemistry**. Vol. 11. pp. 1241-1258

Cossi, M., Rega, N., Scalmani, G. and Barone, V. (2003). Energies, Structures, and Electronic Properties of Molecules in Solution with the C-PCM Solvation Model. **Journal of Computational Chemistry**. Vol. 24. pp. 669-681

Cossi, M. and Barone, V. (2001). Time-dependent density functional theory for molecules in liquid solutions. **Journal of Chemical Physics**. Vol. 115. pp. 4708-4717

Cossi, M., Barone, V., Cammi, R. and Tomasi, J. (1996). Ab initio study of solvated molecules: a new implementation of the polarizable continuum model. **Chemical Physics Letters**. Vol. 255. pp. 327-335

Ding, W.L., Wang, D.M., Geng, Z.Y., Zhao, X.L. and Yan, Y.F. (2013). Molecular Engineering of Indoline-Based D-A-π-A Organic Sensitizers toward High Efficiency Performance from First-Principles Calculations. **J Physical Chemistry C**. Vol. 117. pp. 17382-17398

Ding, W.L., Wang, D.M., Geng, Z.Y., Zhao, X.L. and Xu, W.B. (2013). Density functional theory characterization and verification of high-performance indoline dyes with D-A-π-A architecture for dye-sensitized solar cells. **Dyes and Pigments**. Vol. 98. pp. 125-135

Fischer, M.K.R., Wenger, S., Wang, M., Mishra, A., Zakeeruddin, S.M., Grätzel, M. and Bäuerle, P. (2010). D-π-A Sensitizers for Dye-Sensitized Solar Cells: Linear vs Branched Oligothiophenes. **Chemistry of Materials**. Vol. 22. pp. 1836-1845

Frisch, M.J., Trucks, G.W., Schlegel, H.B., Scuseria, G.E., Robb, M.A., Cheeseman, J.R., Scalmani, G., Barone, V., Mennucci, B., Petersson. G.A., Nakatsuji, H., Caricato, M., Li, X., Hratchian, H.P., Izmaylov, A.F., Bloino, J., Zheng, G., Sonnenberg, J.L., Hada, M., Ehara, M., Toyota, K., Fukuda, R., Hasegawa, J., Ishida, M., Nakajima, T., Honda, Y., Kitao, O., Nakai, H., Vreven, T., Montgomery, Jr.J.A., Peralta, J.E., Ogliaro, F., Bearpark, M., Heyd, J.J., Brothers, E., Kudin, K.N., Staroverov, V.N., Kobayashi, R., Normand, J., Raghavachari, K., Rendell, A., Burant, J.C., Iyengar, S.S., Tomasi, J., Cossi, M., Rega, N., Millam, J.M., Klene, M., Knox, J.E., Cross, J.B., Bakken, V., Adamo, C., Jaramillo, J., Gomperts, R., Stratmann, R.E., Yazyev, O., Austin, A.J., Cammi, R., Pomelli, C., Ochterski, J.W., Martinn, R.L., Morokuma, K., Zakrzewski, V.G., Voth, G.A., Salvador, P., Dannenberg, J.J., Dapprich, S., Daniels, A.D., Farkas, Ö., Foresman, J.B., Ortiz, J.V., Cioslowski, J. and Fox, D.J. (2010). **Gaussian09**. revision B. 01, Gaussian Inc. Wallingford CT.

Gong, J., Liang, J. and Sumathy, K. (2012). Review on dye-sensitized solar cells (DSSCs): Fundamental concepts and novel materials. **Renewable and Sustainable Energy Reviews**. Vol. 16. pp. 5848-5860

Grisorio, R., Marco, L.D., Allegretta, G., Giannuzzi, R., Suranna, G.P., Manca, M., Mastrorilli, P. and Gigli, G. (2013). Anchoring stability and photovoltaic properties of new D(-π-A)$_2$ dyes for dye-sensitized solar cell applications. **Dyes and Pigments**. Vol. 98. pp. 221-231

Hagfeldt, A., Boschloo, G., Sun, L., Kloo, L. and Pettersso, H. (2010). Dye-Sensitized SolarCells. **Chemical Review**. Vol. 110. pp. 6595-6663

Hohenberg, P. and Kohn, W. (1964). Inhomogeneous Electron Gas. **Physical Review B**. Vol. 136. pp. 864-871

Irfan, A. and Al-Sehemi, A.G. (2012). Quantum chemical study in the direction to design efficient donor-bridge-acceptor triphenylamine sensitizers with improved electron injection. Journal of Molecular Modeling. Vol. 18. pp. 4893-4900

Ito, S., Zakeeruddin, S.M., Humphry-Baker, R., Liska, P., Charvet, R., Comte, P., Nazeeruddin, M.K., Péchy, P., Takata, M., Miura, H., Uchida, S. and Grätzel, M. (2006). High-Efficiency Organic-Dye-Sensitized Solar Cells Controlled by Nanocrystalline-TiO_2 Electrode Thickness. Advanced Materials. Vol. 18. pp. 1202-1205

Kim, B.H. and Freeman, H.S. (2013). New N-methyl pyrrole and thiophene based D-π-A systems for dye-sensitized solar cells. Dyes and Pigments. Vol. 96. pp. 313-318

Khon, W. and Sham, L. (1965). Self-Consistent Equations Including Exchange and Correlation Effects. J Physical Review A. Vol. 140. pp. 1133-1138

Lee, C., Yang, W. and Parr, R. (1988). Development of the Colle-Salvetti correlation energy formula into a functional of the electron density. Physical Review B. Vol. 37. pp. 785-789

Menzel, R., Ogermann, D., Kupfer, S., Wei, D., Görls, H., Kleinermanns, K., Gonzölez, L. and Beckert, R. (2012). 4-Methoxy-1,3-thiazole based donor-acceptor dyes: Characterization, X-ray structure, DFT calculations and test as sensitizers for DSSC. Dyes and Pigments. Vol. 94. pp. 512-524

O'Regan, B. and Gratzel, M. (1991). A low-cost, high-efficiency solar cell based on dye-sensitized colloidal TiO_2 films. Nature. Vol. 353. pp. 737-74

Parr, R.G. and Young, W. (1989). Density Functional Theory of Atoms and Molecules. Oxford University Press, Oxford, UK

Sang-aroon, W., Saekow, S. and Amornkitbamrung, V. (2013). DFT and TDDFT study on the electronic structure and photoelectrochemical properties of dyes derived from cochineal and lac insects as photosensitizer for dye-sensitized solar cells. Journal of Molecular Modeling. Vol. 19. pp. 1407-1415

Sang-aroon, W., Saekow, S. and Amornkitbamrung, V. (2012). Density functional theory study on the electronic structure of Monascus dyes as photosensitizer for dye-sensitized solar cells. Journal of Photochemistry and Photobiology A: Chemistry. Vol. 236. pp. 35-40

Sirohi, R., Kim, D.H., Yu, S.C. and Lee, S.H. (2012). Novel di-anchoring dye for DSSC by bridging of two mono anchoring dye molecules: A conformational approach to reduce aggregation. Dyes and Pigments. Vol. 92. pp. 1132-1137

Snaith, H.J. (2010). Estimating the Maximum Attainable Efficiency in Dye-Sensitized Solar Cells. Journal of Advanced Functional Materials. Vol. 20. pp. 13-19

Tarsang, R., Promarak, V., Sudyoadsuk, T., Namuangruk, S. and Jungsuttiwong, S. (2014). Tuning the electron donating ability in the triphenylamine-based D-π-A architecture for highly efficient dye-sensitized solar cells. **Journal of Photochemistry and Photobiology A: Chemistry**. Vol. 273. pp. 8-16

Verbitskiy, E.V., Cheprakova, E.M., Subbotina, J.O., Schepochkin, A.V., Slepukhin, P.A., Rusinov, G.L., Charushin, V.N., Chupakhin, O.N., Makarova, N.I., Metelitsa, A.V. and Minkin, V.I. (2014). Synthesis, spectral and electrochemical properties of pyrimidine-containing dyes as photosensitizers for dye-sensitized solar cells. **Dyes and Pigments**. Vol. 100. pp. 201-214

Wu, C.G., Shieh, W.T., Yang, C.S., Tan, C.J., Chang, C.H., Chen, S.C., Wu, C.Y. and Tsai, H.H.G. (2013). Molecular Engineering of Indoline-Based D-A-π-A Organic Sensitizers toward High Efficiency Performance from First-Principles Calculations. **Dyes and Pigments**. Vol. 99. pp. 1091-1100

Yanai, T., Tew, D.P. and Handy, N.C. (2004). A new hybrid exchange-correlation functional using the Coulomb-attenuating method (CAM-B3LYP). **Chemical Physics Letters**. Vol. 393. pp. 51-57